View metadata, citation and similar papers at core.ac.uk

brought to you by CORE

provided by Vietnam Academy of Science and Technology: Journals Online

Vietnam Journal of Science and Technology ***57*** *(6) (2019) 749-761*

doi:10.15625/2525-2518/57/6/13838

SOUND TRANSMISSION LOSS ACROSS A FINITE SIMPLY SUPPORTED DOUBLE-LAMINATED COMPOSITE PLATE WITH ENCLOSED AIR CAVITY

Pham Ngoc Thanh[1, *], Tran Ich Thinh[2]

[1]*Viettri University of Industry, Street Hung Vuong, Viet Tri, Phu Tho*

[2]*Hanoi University of Science and Technology, Street Dai Co Viet, Hai Ba Trung, Ha Noi*

Email: *thanhpham1986@gmail.com*

Received: 24 May 2019; Accepted for publication: 11 November 2019

Abstract. Vibro-acoustic analysis of a finite orthotropic laminated double-composite plate with enclosed air cavity on an infinite acoustic rigid baffle is investigated analytically. Using the acoustic velocity potential to describe the acoustic vibration performance of a simple supported structure, the sound transmission loss (STL) is calculated from the ratio of incident to transmitted acoustic powers. Specifically, the focus is placed on the effects of several key system parameters on sound transmission including the plate dimensions, the laminate configurations, the boundary conditions and the composite materials are systematically examined.

Keywords: double-composite plate, orthotropic faceplate, simply supported boundary condition.

Classification numbers: 2, 2.9, 2.9.4.

1. INTRODUCTION

With the superior sound insulation characteristics of the double-plate compared to a single plate, the double-plate is increasingly widely used as in construction structures, ships, turbofan, aerospace, automobiles, etc. Therefore, research on sound insulation capacity of the double-plate has received much attention from researchers in the world to produce the most optimal structures with the best sound insulation ability and the best applicability.

For decades, the sound transmission loss across an infinite or finite double-plates is an interesting research topic with the different approaches used. Traditionally, Maidanik [1] analyzed the vibration behavior of a complex structure under force or sound excitation by the statistical energy analysis method (SEA). However, the SEA method is less effective at relatively low frequencies on account of its pre-assumption that enough structural modes need to be excited. Ruzzene [2] investigated the acoustic properties of sandwich beams in terms of structural response and sound transmission reduction index, which is more efficient for low frequencies but required high calculation costs for high frequencies by a finite element method model (FEM). London [3] has conducted the first experiment of sound insulation for double plate structure. Later, Carneal and Fuller [4] studied an analytical and experimental of active

structural acoustic control of sound transmission across aluminium double-plate systems. Chazot and Guyader [5] used the patch-mobility method to investigate the sound transmission loss through finite double-panels. The actual results are quite similar when compared with the FEM method. However, the path-mobility method allows for research in a wider frequency range. In addition, Bao and Pan [6] performed an experimental study of different approaches for active control of sound transmission through double walls. Sgard et al. [7] studied the sound transmission loss through a finite double-plate lined with poroelastic material by FEM. Villot et al. [8] have proposed a new way for calculating the reflectance and transmitting power of finite multi-layered structures based on spatial widowing of plane waves.

Nowadays, to reduce vibration and control noise, we use double-plates filled with absorbing materials. The study of sound transmission loss through a sandwich structure is getting more and more attention from domestic and foreign researchers. Brouard et al. [9] presented a general method for sound transmission through fluid-saturated porous layers. Based on Biot model, Lauriks et al. [10] have proposed a transfer matrix model for acoustic transmission through double-plate filled with porous material. By finite element method, Larbi et al. [11] studied the sound transmission through double wall sandwich panels with viscoelastic core. Panneton and Atalla [12] investigated a three-dimensional (3D) finite element model to calculate the sound transmission loss through multilayer structures containing porous absorbent materials. The structures considered vary according to whether the filling porous material is bonded or not to the faceplates. Chonan and Kugo [13] proposed a model to evaluate the sound propagation properties of a flane wave through a three-layered plate using two-dimensional (2D) elasticity theory. Kang et al. [14] used the method of Gauss distribution function for investigating the STL of multilayered plates such as double-plate structures embedded with porous materials. Bolton et al. [15] calculated sound transmission through multi-plate structures lined with elastic porous materials.

More recently, the problem of sound transmission across a finite double-plate structures was investigated with a simple supported boundary [16, 17] on the basis from different perspectives. Lu and Xin [17] presented the sound transmission across rectangular metallic double-panel structure with an air cavity with various boundary constraints by using the modal function and the Galerkin method. Numerous analytical investigations on the STL through a finite isotropic (metallic) double-plate have been performed [8, 10, 13]. However, there are only a few studies on the sound transmission loss across a finite simply supported double-composite plate. Thinh and Thanh studied the sound transmission loss through a finite clamped single composite plate [18].

The present study has expanded a model to calculate the sound transmission across a finite simply supported laminated double-composite plate with enclosed air cavity. The effect of several key system parameters on STL of this composite structure (e.g., the plate dimensions, the laminate configurations, the boundary conditions and the surface density of composite materials) is systematically examined.

2. VIBROACOUSTIC COUPLED SYSTEM MODELING

2.1. Geometry and assumption

Supposedly, a finite rectangular double-composite plate with air cavity is in an infinite large acoustic rigid baffle. The two single-plates are orthotropic laminated composite and have similar geometric parameters and mechanical properties. The bottom and upper face plates (Fig.

1) have the same thickness h and is separated by an air cavity of thickness H. The double-plate partition divides the space into two fields, i.e., sound incidence field ($z < 0$) and sound transmitting field ($z > H+2h$).

A plane sound wave varying harmonically in time is oblique (with the incident angle φ and azimuth angle θ) and stimulates the vibration of the bottom plate. This vibration changes the pressure in the air cavity and causes vibration of the upper plate then the sound wave is transmitted into the upper domain.

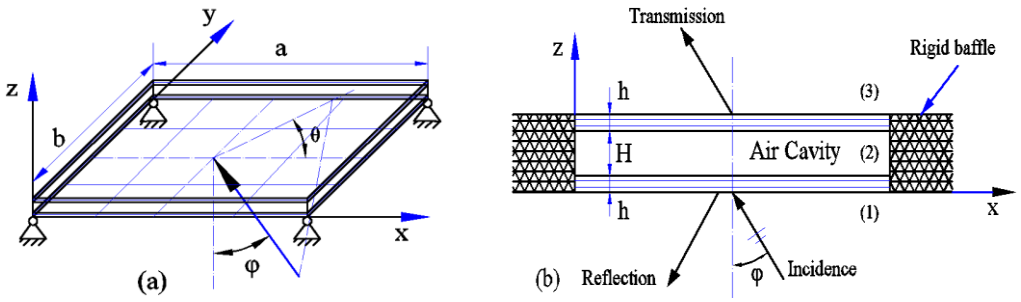

Figure 1. Schematic of a simply supported composite double-plate: (a) Global view and (b) Side view.

2.2. Theoretical formulation

Based on the classical plate theory, the vibroacoustic behavior of an orthotropic symmetric laminated double-composite plate with enclosed air cavity (Fig. 1) induced by sound wave excitation is governed by [18, 19, 20, 21]:

$$D_{11}\frac{\partial^4 w_1(x,y;t)}{\partial x^4}+2(D_{12}+2D_{66})\frac{\partial^4 w_1(x,y;t)}{\partial x^2\partial y^2}+D_{22}\frac{\partial^4 w_1(x,y;t)}{\partial y^4}+m^*\frac{\partial^2 w_1(x,y;t)}{\partial^2 t}-j\omega\rho_0[\Phi_1(x,y,z;t)-\Phi_2(x,y,z;t)]=0 \quad (1)$$

$$D_{11}\frac{\partial^4 w_2(x,y;t)}{\partial x^4}+2(D_{12}+2D_{66})\frac{\partial^4 w_2(x,y;t)}{\partial x^2\partial y^2}+D_{22}\frac{\partial^4 w_2(x,y;t)}{\partial y^4}+m^*\frac{\partial^2 w_2(x,y;t)}{\partial^2 t}-j\omega\rho_0[\Phi_2(x,y,z;t)-\Phi_3(x,y,z;t)]=0 \quad (2)$$

where $w_{1,2}$ are the transverse displacements of the upper and bottom faceplates; D_{ij} (ij = 11, 12, 22, 66) are the flexural rigidities; m^* is the surface density of the upper and bottom plates; ρ_0 is the air density, ω is the angular frequency of the incident sound and Φ_i (i = 1, 2, 3) are the acoustic velocity potentials for the incident field, the air cavity, and the transmitting field, respectively.

The flexural rigidity of the laminated composite plate is given by (see any textbook of Mechanics of composite materials):

$$D_{ij}=\frac{1}{3}\sum_{k=1}^{n}Q_{ij}^{k}\left(z_{k+1}^3-z_k^3\right) \quad (3)$$

where Q_{ij} are the reduced stiffnesses of the k^{th} layer and are defined as:

$$Q_{11}=\frac{E_1}{1-\nu_{12}\nu_{21}};Q_{12}=\frac{\nu_{12}E_1}{1-\nu_{12}\nu_{21}};Q_{22}=\frac{E_2}{1-\nu_{12}\nu_{21}};Q_{66}=G_{12};\frac{\nu_{12}}{E_1}=\frac{\nu_{21}}{E_2} \quad (4)$$

and E_1, E_2, G_{12}, ν_{12} are the k^{th} layer elastic constants.

For isotropic plates, $D_{11} = D_{22} = Eh^3/[12(1-\nu^2)]$, $D_{12} = \nu D_{11}$, $D_{66} = Gh^3/12$.

The displacements of the bottom and upper faceplates induced by the incident sound is given by:

$$w_1(x,y;t) = w_{01}.e^{-j(k_x x+k_y y-\omega t)};\ w_2(x,y;t) = w_{02}.e^{-j(k_x x+k_y y-\omega t)} \tag{5}$$

The acoustic velocity potential in the incidence field (*Fig.1*) can be expressed by [10, 16, 17]:

$$\Phi_1(x,y,z;t) = I.e^{-j(k_x x+k_y y+k_z z-\omega t)} + \beta.e^{-j(k_x x+k_y y-k_z z-\omega t)} \tag{6}$$

where I and β are the amplitudes of the incident (positive-going) and the reflected plus radiated (negative-going) waves, respectively. Similarly, the velocity potential in the air cavity can be written as:

$$\Phi_2(x,y,z;t) = \varepsilon.e^{-j(k_x x+k_y y+k_z z-\omega t)} + \psi.e^{-j(k_x x+k_y y-k_z z-\omega t)} \tag{7}$$

where ε is the amplitude of the positive-going wave and ψ is the amplitude of the negative-going wave. In the transmitted field adjacent to the transmitting upper plate, there exist no reflected waves, and therefore the velocity potential in the transmitted waves is given by:

$$\Phi_3(x,y,z;t) = \gamma.e^{-j(k_x x+k_y y+k_z z-\omega t)} \tag{8}$$

where γ is the amplitude of the transmitted wave.

These wavenumbers are determined by the incident angle φ and azimuth angle θ of the incident field as:

$$k_x = k_0 \sin\varphi\cos\theta; k_y = k_0 \sin\varphi\sin\theta; k_z = k_0\cos\varphi \tag{9}$$

where $k_0 = \omega/c_0$ is the wave number in the air and c_0 is the sound speed in the air.

The boundary conditions for the simply supported double-composite plate can be obtained:

$$\text{at } x = 0 \text{ and } a,\ w_1 = w_2 = 0,\ \frac{\partial^2 w_1}{\partial x^2} = \frac{\partial^2 w_2}{\partial x^2} = 0;\ \text{at y} = 0 \text{ and b},\ \text{w}_1 = w_2 = 0, \frac{\partial^2 \text{w}_1}{\partial \text{y}^2} = \frac{\partial^2 \text{w}_2}{\partial \text{y}^2} = 0 \tag{10}$$

At the air-plate interface, the normal velocity is continuous, yielding the corresponding velocity compatibility condition equations

$$z = 0,\ -\frac{\partial \Phi_1}{\partial z} = j\omega w_1;\ \text{z} = \text{h},\ -\frac{\partial \Phi_2}{\partial z} = j\omega w_1;\ z = h + H,\ -\frac{\partial \Phi_2}{\partial z} = j\omega w_2;\ \text{z} = 2\text{h} + \text{H},\ -\frac{\partial \Phi_3}{\partial z} = j\omega w_2 \tag{11}$$

The flexural motions of the bottom and upper plates induced by a time-harmonic incident plate sound wave can be expressed in the form of double series as:

$$w_1(x,y;t) = \sum_{m=1}^{\infty}\sum_{n=1}^{\infty}\varphi_{mn}(x,y)u_{1,mn}(t);\ w_2(x,y;t) = \sum_{m=1}^{\infty}\sum_{n=1}^{\infty}\varphi_{mn}(x,y)u_{2,mn}(t) \tag{12}$$

where the modal function φ_{mn} and modal displacements $u_{i,mn}$ (i = 1, 2) for simply supported boundary conditions are given by [20]:

$$\varphi_{mn}(x,y) = \sin\left(\frac{m\pi x}{a}\right)\sin\left(\frac{n\pi y}{b}\right) \tag{13}$$

$$u_{1,mn}(t) = \alpha_{1,mn}e^{j\omega t},\ u_{2,mn}(t) = \alpha_{2,mn}e^{j\omega t} \tag{14}$$

where $\alpha_{1,mn}$; $\alpha_{2,mn}$ are the modal coefficients of the bottom and upper plates, respectively.

Thus, the velocity potentials for the sound incident field, air cavity, and sound transmitting field are given by:

$$\Phi_1(x,y,z;t)=\sum_{m,n=1}^{\infty} I_{mn}\varphi_{mn}e^{-j(k_z z-\omega t)}+\sum_{m,n=1}^{\infty}\beta_{mn}\varphi_{mn}e^{-j(-k_z z-\omega t)} \tag{15}$$

$$\Phi_2(x,y,z;t)=\sum_{m,n=1}^{\infty} \varepsilon_{mn}\varphi_{mn}e^{-j(k_z z-\omega t)}+\sum_{m,n=1}^{\infty}\psi_{mn}\varphi_{mn}e^{-j(-k_z z-\omega t)} \tag{16}$$

$$\Phi_3(x,y,z;t)=\sum_{m,n=1}^{\infty} \gamma_{mn}\varphi_{mn}e^{-j(k_z z-\omega t)} \tag{17}$$

where the coefficients I_{mn}, β_{mn}, ε_{mn}, ψ_{mn} and γ_{mn} for simply supported double-composite plate are determined by:

$$\Omega_{mn}=\frac{4}{ab}\int_0^b\int_0^a \Omega e^{-j(k_x x+k_y y)}\sin\frac{m\pi x}{a}\sin\frac{n\pi x}{b}dxdy \tag{18}$$

here, the symbol Ω can be coefficients I, β, ε, ψ and γ.

2.3. Determination of modal coefficients of the bottom and upper plates

Let ξ_1, ξ_2, and ξ_3 represent the acoustic particle displacement in the incident field, the air cavity and the transmitted field, respectively. The air particle displacement and the sound pressure are related by the air momentum equation, as [22]:

$$\frac{\partial^2}{\partial t^2}\xi_1=-\frac{1}{\rho_0}\frac{\partial p_1}{\partial z}\bigg|_{z=0};\ \frac{\partial^2}{\partial t^2}\xi_2=-\frac{1}{\rho_0}\frac{\partial p_2}{\partial z}\bigg|_{z=h};\ \frac{\partial^2}{\partial t^2}\xi_2=-\frac{1}{\rho_0}\frac{\partial p_2}{\partial z}\bigg|_{z=h+H};\ \frac{\partial^2}{\partial t^2}\xi_3=-\frac{1}{\rho_0}\frac{\partial p_3}{\partial z}\bigg|_{z=H+2h} \tag{19}$$

where p_i *(i = 1,2,3)* is the acoustic pressure that can be expressed by the Bernoulli equation, as [23]:

$$p_i=\rho_0\left[\frac{\partial\Phi_i}{\partial t}\right]\quad (\mathrm{i}=1,2,3) \tag{20}$$

The displacements of the air particle adjacent to the plate in each region can be expressed as

$$\xi_1=\xi_{10}e^{-j(k_x x+k_y y-\omega t)}\Big|_{z=0};\ \xi_2=\xi_{20}e^{-j(k_x x+k_y y-\omega t)}\Big|_{z=h};\ \xi_2=\xi_{30}e^{-j(k_x x+k_y y-\omega t)}\Big|_{z=h+H};\ \xi_3=\xi_{30}e^{-j(k_x x+k_y y-\omega t)}\Big|_{z=2h+H} \tag{21}$$

Replace the equations (20) and (21) into (19), and applying equations (6) and (8), one can obtain:

$$\xi_{10}=\left(\sum_{m=1}^{\infty}\sum_{n=1}^{\infty}I_{mn}\varphi_{mn}-\sum_{m=1}^{\infty}\sum_{n=1}^{\infty}\beta_{mn}\varphi_{mn}\right)\frac{k_z}{\omega}e^{j(k_x x+k_y y)};\ \xi_{20}=\left(\sum_{m=1}^{\infty}\sum_{n=1}^{\infty}\varepsilon_{mn}\varphi_{mn}-\sum_{m=1}^{\infty}\sum_{n=1}^{\infty}\psi_{mn}\varphi_{mn}\right)\frac{k_z}{\omega}e^{j(k_x x+k_y y)} \tag{22}$$

$$\xi_{30}=\sum_{m=1}^{\infty}\sum_{n=1}^{\infty}\gamma_{mn}\varphi_{mn}\frac{k_z}{\omega}e^{j(k_x x+k_y y)} \tag{23}$$

The factual case that the composite plate immersed in an air medium requires that the displacements of the air particles adjacent to the panel should be the same as those of the attached plate particles. Accordingly, the displacement continuity condition can be written as:

$$\xi_{10}=w_{01}\big|_{z=0};\ \xi_{20}=w_{01}\big|_{z=h};\ \xi_{20}=w_{02}\big|_{z=h+H};\ \xi_{30}=w_{02}\big|_{z=2h+H} \tag{24}$$

The substitution of Eqs. (15) - (17) into Eqs. (11) leads to:

$$\beta_{mn} = I_{mn} - \frac{\omega}{k_z}\alpha_{1,mn} \;;\; \varepsilon_{mn} = \frac{\omega\left(\alpha_{1,mn}e^{jk_zH} - \alpha_{2,mn}\right)}{k_z\left(e^{-jk_z(h-H)} - e^{-jk_z(H+h)}\right)} \tag{25}$$

$$\psi_{mn} = \frac{\omega\left(\alpha_{2,mn} - \alpha_{1,mn}e^{-jk_zH}\right)}{k_z\left(e^{jk_z(h-H)} - e^{jk_z(H+h)}\right)};\; \gamma_{mn} = \frac{\omega\alpha_{2,mn}e^{jk_z(H+2h)}}{k_z} \tag{26}$$

Substituting equations (12), (25) and (26) into equations (1) and (2) and applying the orthogonal functions, one gets:

$$\ddot{u}_{1,mn}(t) + \omega_{1,mn}^2 u_{1,mn}(t) - \frac{j\omega\rho_0}{m^*}\left[\left(I_{mn} - \varepsilon_{mn}\right)e^{-j(k_zz-\omega t)} + \left(\beta_{mn} - \psi_{mn}\right)e^{-j(-k_zz-\omega t)}\right] = 0 \tag{27}$$

$$\ddot{u}_{2,mn}(t) + \omega_{2,mn}^2 u_{2,mn}(t) - \frac{j\omega\rho_0}{m^*}\left[\left(\varepsilon_{mn} - \gamma_{mn}\right)e^{-j(k_zz-\omega t)} + \psi_{mn}e^{-j(-k_zz-\omega t)}\right] = 0 \tag{28}$$

The natural frequencies of two faceplates are determined by [24]:

$$\omega_{i,mn}^2 = \frac{\iint_A \left(D_{11}\frac{\partial^4\varphi_{mn}}{\partial^4 x} + 2\left(D_{12} + 2D_{66}\right)\frac{\partial^4\varphi_{mn}}{\partial^2 x\partial^2 y} + D_{22}\frac{\partial^4\varphi_{mn}}{\partial^4 y}\right).\varphi_{mn}dA}{m^*\iint_A \varphi_{mn}.\varphi_{mn}dA}\left(i = 1,2\right)$$

$$\Leftrightarrow \omega_{i,mn}^2 = \frac{\pi^4}{m^*b^4}\left[D_{11}m^4\left(\frac{b}{a}\right)^4 + 2\left(D_{12} + 2D_{66}\right)m^2n^2\left(\frac{b}{a}\right)^2 + D_{22}n^4\right]\left(i = 1,2\right) \tag{29}$$

Combine the equations (14), (27) and (28) can be rewritten in matrix form as:

$$\begin{bmatrix} X_{11} & X_{12} \\ X_{21} & X_{22} \end{bmatrix}\begin{Bmatrix} \alpha_{1,mn} \\ \alpha_{2,mn} \end{Bmatrix} = \begin{Bmatrix} Y \\ 0 \end{Bmatrix} \tag{30}$$

where:

$$\begin{aligned}
X_{11} &= \omega_{1,mn}^2 - \omega^2 - \frac{j\omega^2\rho_0}{k_zm^*}\left[\frac{e^{jk_zH}}{e^{-jk_z(h-H)} - e^{-jk_z(H+h)}} - \frac{e^{-jk_zH}}{e^{jk_z(h-H)} - e^{jk_z(H+h)}}\right] \\
X_{12} &= \frac{j\omega^2\rho_0}{k_zm^*}\left[\frac{1}{e^{-jk_z(h-H)} - e^{-jk_z(H+h)}} - \frac{1}{e^{jk_z(h-H)} - e^{jk_z(H+h)}}\right] \\
X_{21} &= \frac{j\omega^2\rho_0}{k_zm^*}\left[\frac{e^{jk_zH}}{e^{-jk_z(h-H)} - e^{-jk_z(H+h)}} - \frac{e^{-jk_zH}}{e^{jk_z(h-H)} - e^{jk_z(H+h)}}\right] \\
X_{22} &= \omega_{2,mn}^2 - \omega^2 - \frac{j\omega^2\rho_0}{k_zm^*}\left[\frac{1}{e^{jk_z(h-H)} - e^{jk_z(H+h)}} - \frac{1}{e^{-jk_z(h-H)} - e^{-jk_z(H+h)}} + e^{jk_z(H+2h)}\right] \\
Y &= \frac{2j\omega\rho_0 I_{mn}}{m^*}
\end{aligned} \tag{31}$$

After solving the system of equations (30), we determine the coefficients $\alpha_{1,mn}$ and $\alpha_{2,mn}$ from which we determine other quantities such as w_1, w_2 and the coefficients (β_{mn}, ε_{mn}, ψ_{mn} and γ_{mn}). So, the analysis of sound transmission loss through a simply supported double-composite plate is completely solved.

3. CACULATION OF SOUND TRANSMISSION LOSS

The power of incident sound is defined by [12, 17]:

$$\Pi_1 = \frac{1}{2}\mathrm{Re}\iint_A p_1 v_1^* dA \tag{32}$$

where $v_1^* = p_1/(\rho_0 c_0)$ is the local acoustic velocity, and

$$p_1 = j\rho_0\omega\Phi_1(x,y,0) = j\rho_0\omega\left[2Ie^{-j(k_x x+k_y y)} - \sum_{m,n=1}^{\infty}\frac{\omega}{k_z}\alpha_{1,mn}\varphi_{mn}(x,y)\right] \tag{33}$$

is the sound pressure in the incident field. Substitution p_1 and v_1^* into (32) yields:

$$\Pi_1 = \frac{\rho_0\omega^2}{2c_0}\left|4I^2\iint_A e^{-2j(k_x x+k_y y)}dA - 4I\frac{\omega}{k_z}\sum_{m,n=1}^{\infty}\alpha_{1,mn}\iint_A e^{-j(k_x x+k_y y)}\sin\left(\frac{m\pi x}{a}\right)\sin\left(\frac{n\pi y}{b}\right)dA\right. \\ \left. + \frac{\omega^2}{k_z^2}\sum_{m,n=1}^{\infty}\sum_{k,l=1}^{\infty}\alpha_{1,mn}\alpha_{1,kl}\iint_A \sin\left(\frac{m\pi x}{a}\right)\sin\left(\frac{n\pi y}{b}\right)\sin\left(\frac{k\pi x}{a}\right)\sin\left(\frac{l\pi y}{b}\right)dA\right| \tag{34}$$

The transmitted sound power is given by [12, 17]:

$$\Pi_3 = \frac{1}{2}\mathrm{Re}\iint_A p_3 v_3^* dA \tag{35}$$

where $v_3^* = p_3/(\rho_0 c_0)$ is the local acoustic velocity and

$$p_3 = j\rho_0\omega\Phi_3(x,y,0) = j\rho_0\frac{\omega^2}{k_z}\sum_{m=1}^{\infty}\sum_{n=1}^{\infty}\alpha_{2,mn}\varphi_{mn}(x,y) \tag{36}$$

is the sound pressure in the transmitted field. Combination of Eqs. (35) and (36) and the expression of v_3^* results in:

$$\Pi_3 = \frac{\rho_0\omega^4}{2c_0k_z^2}\left|\sum_{m,n=1}^{\infty}\sum_{k,l=1}^{\infty}\alpha_{2,mn}\alpha_{2,kl}\iint_A \sin\left(\frac{m\pi x}{a}\right)\sin\left(\frac{n\pi y}{b}\right)\sin\left(\frac{k\pi x}{a}\right)\sin\left(\frac{l\pi y}{b}\right)dA\right| \tag{37}$$

The sound transmission loss across the laminated double-composite plate is defined by [12]:

$$STL = 10\log_{10}\left(\frac{\Pi_1}{\Pi_3}\right). \tag{38}$$

4. NUMERICAL RESULTS AND DISCUSSION

4.1. Validation

For validation, the present analytical solutions are compared with the experimental results of Lu and Xin [17] for a simply supported double-plate, as shown in Fig. 2. The double-plate considered consists of two identical aluminum (isotropic) faceplates. The dimensions of the plates are: length of the plate a = 0.3 m, width of the plate b = 0.3 m. The faceplate has thickness h = 0.001 m while the thickness of the air cavity is H = 0.08 m. The mechanical properties of aluminum materials are: E = 70 GPa; ρ = 2700 kg/m^3; ν = 0.33. The air speed of sound, c = 343 m/s; ρ_0 = 1.21 kg/m^3; the amplitude of the acoustic velocity potential for the incident sound is I_0 = 1 m^2/s.

Looking at Figure 2, we can see that the current predictions are closely matched with the experimental measurements of [17]. The obvious difference between theory and experiment is attributed to a number of factors such as the incident wave has not satisfied the condition of a plane wave or the connection of the structure or due to interference between waves during the experiment. Note also that the experimental results at frequencies below 50 Hz are not reliable because the flanking transmission paths of the test facility play a prominent role in this frequency range. The results of Fig. 2 clearly demonstrate the intense peaks and dips in the STL versus frequency curve reflect the inherent modal behaviors of the double-panel system. It should be pointed out that the STL dips (apart from the second dips in the two theoretical curves) are dominated by the modal behavior of the radiating plate. It has been established that the second dips are associated with the "plate-cavity-plate" resonance, which is insensitive to the imposed boundary condition.

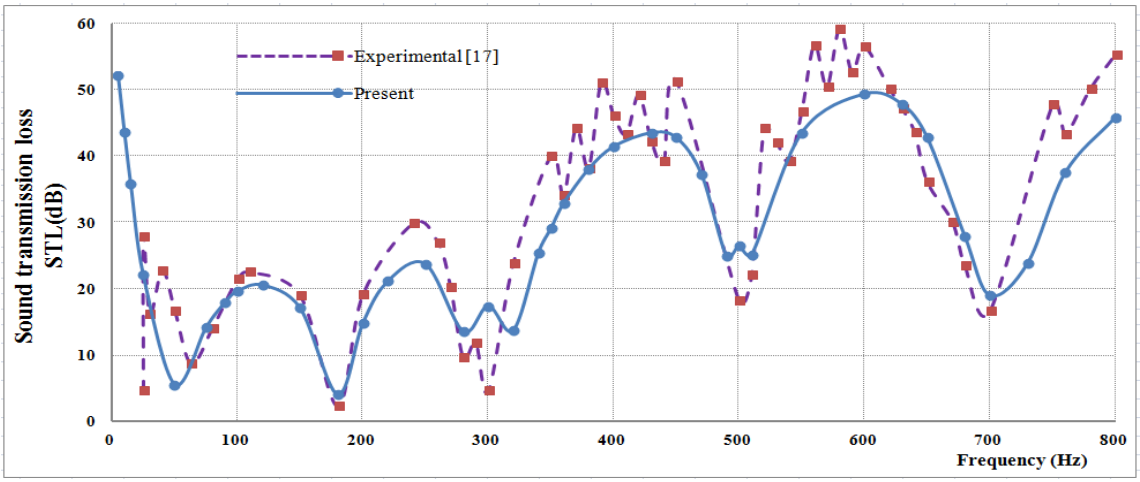

Figure 2. Comparison of STL between the present prediction and experimental result of [17].

4.2. Effects of the plate dimensions on sound transmission loss

In this section, numerical calculations are carried out to consider the influence of faceplate dimensions on STL of a finite simply supported double-composite plate with enclosed air cavity. Four double-composite plates: 1 × 1 m^2; 4 × 4 m^2; 16 × 16 m^2 and 100× 100 m^2 are chosen. The bottom and upper faceplates are graphite/epoxy with the plies being arranged in a $[0/90/0/90]_s$ pattern and the mechanical properties:

$$E_1 = 137 \text{ GPa}; E_2 = 10 \text{ GPa}; G_{12} = 5 \text{ GPa}; \nu_{12} = 0.30; \rho = 1590 \text{ kg/m}^3.$$

The other geometric parameters are presented in above section 4.1.

The results in Figure 3 show that, when increasing the dimensions of a finite plate to a certain extent, the plate is considered to be infinite and in this case so, with the size 100x100 m^2, the plate can be considered infinite. For finite double plates, the initial behavior of the upper and lower plates interact strongly with system behavior (including plate-air cavity-plate resonance and standing wave resonance), which plays a major role in the vibration of all system. However, for infinite double plates the behavior of the original mode does not affect the negative oscillation behavior of the whole system. Results obtained, only dips related to system resonances show up in Fig. 3, with the first dip representing the mass-air-mass resonance and the

remaining dips caused by the standing-wave resonance. Over a wide frequency range, the maximum and dip points in the STL curve of the finite plate have a higher modal density than the infinite plate. Conversely in the low frequency range no mode exists for finite plates. In other words, the infinite plate is incapable of providing the right STL values at low frequencies for the practical finite plate.

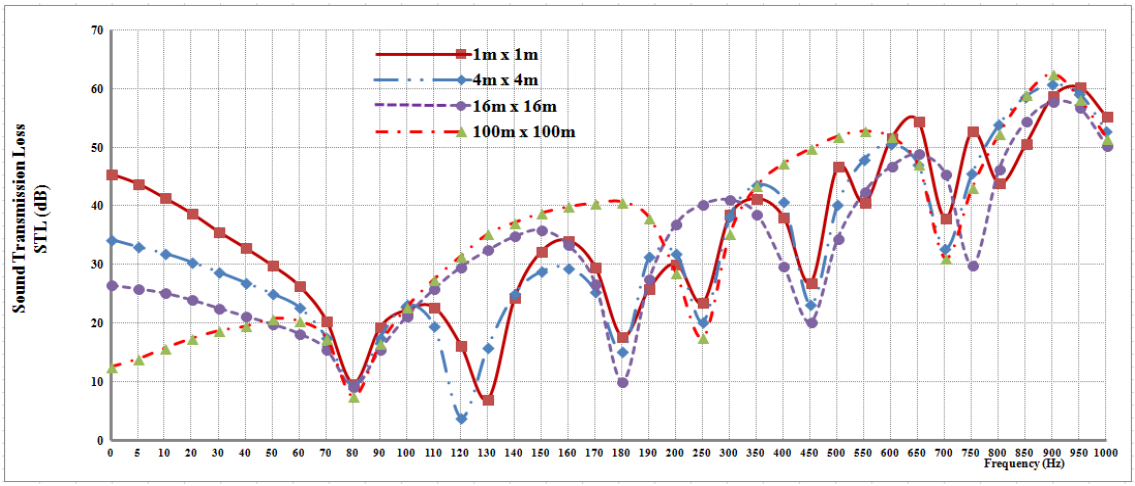

Figure 3. Influence of the plate dimension on STL of a simply supported double-composite plate with enclosed air cavity.

4.3. Effects of laminate configurations on sound transmission loss

In order to quantify the effects of lamination scheme on STL through the double-composite plate with an enclosed air cavity, four following configurations of the bottom and upper Graphite/epoxy composite plates are selected: $[0/90/0/90]_s$, $[0/0/0/0]_s$, $[90/90/90/90]_s$ and $[90/0/0/90]_s$. The length of the plate a = 1 m and the width of the plate b = 1 m. The faceplates have thickness h = 0.005 m while the thickness of the air cavity is H = 0.08 m.

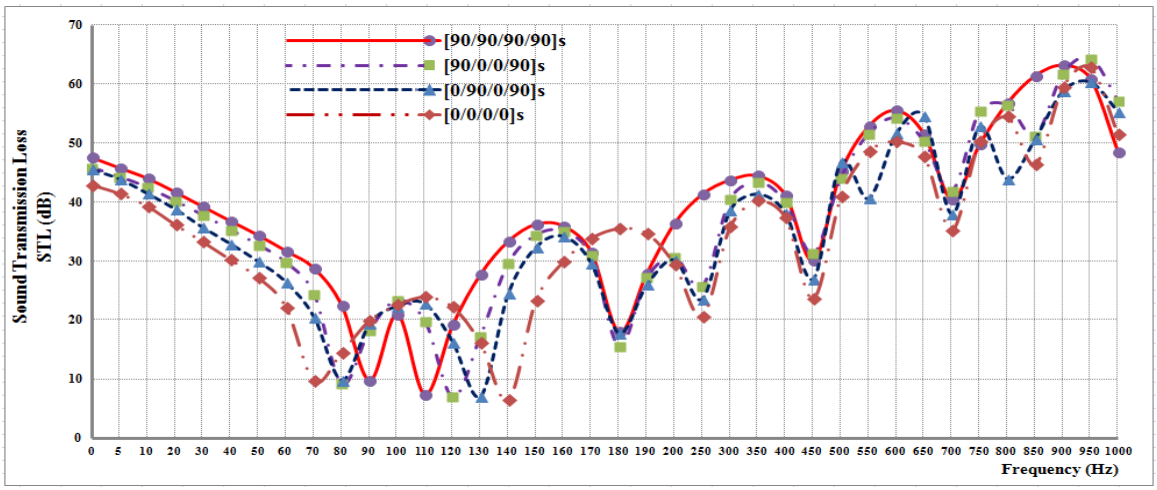

Figure 4. Influence of laminate configuration on STL of a simply supported double-composite plate with enclosed air cavity.

As can be seen from Fig. 4, the lamination scheme [90/90/90/90]s has enhanced the STL better than the other patterns for all ranges of considered frequency.

4.4. Effects of different boundary conditions on sound transmission loss

In this section, the STL is calculated for two double-composite plates subjected to clamped and simply supported boundary conditions, respectively. The results are compared for the sound incident with elevation angle, $\varphi = 30^o$ and azimuth angle, $\theta = 30^o$.

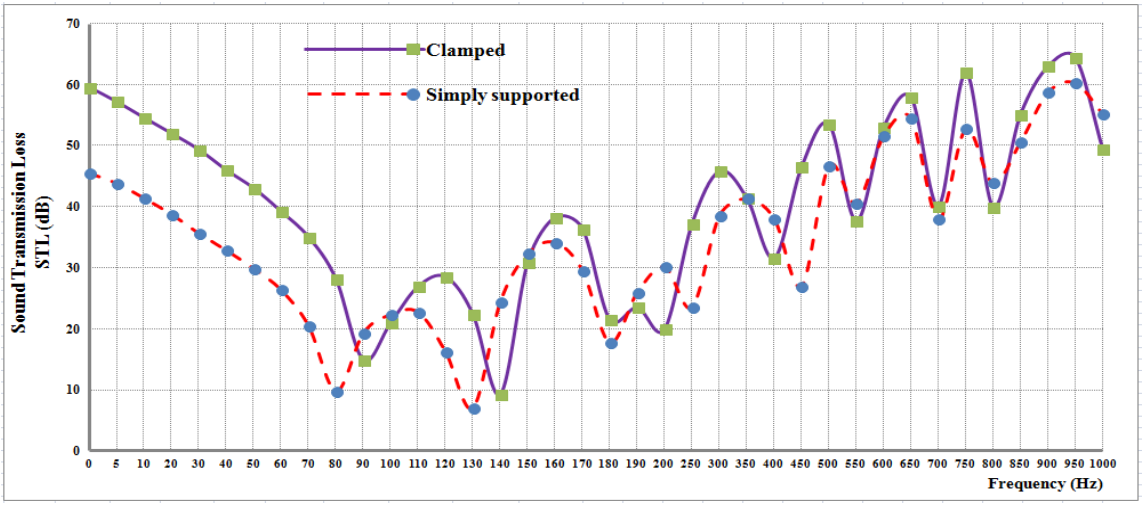

Figure 5. Compared the sound transmission loss of a finite double-composite plate with clamped boundary and simply supported boundary.

One can see in Fig. 5 that the first dip is very sensitive to the flexural stiffness of the plate and the second dip (i.e., plate-air cavity-plate resonance) is not sensitive to the boundary conditions (clamped and simply supported). It can be seen that the STL values of the clamped system are distinctly higher than those of the simply supported system in whole frequency range. The STL values obtained with the two different boundary conditions have overall the same order of magnitude, although the resonance dips are not in accord with each other.

4.5. Effect of composite materials on sound transmission loss

Table 1. Composite materials properties.

Composite	E_1 *(GPa)*	E_2 *(GPa)*	G_{12} *(GPa)*	v_{12}	ρ *(Kg/m3)*
Boron/Epoxy	204.000	18.500	5.590	0.23	2000
Glass/Epoxy	40.851	10.097	3.788	0.27	1946
Graphite/Epoxy	181.000	10.300	7.170	0.28	1600
Kevlar/Epoxy	76.000	5.500	2.300	0.34	1460

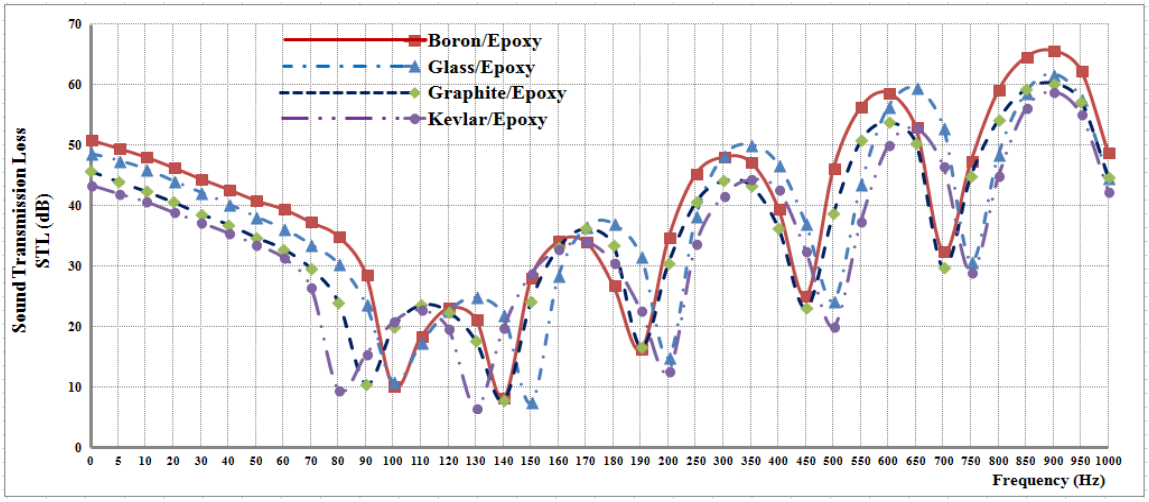

Figure 6. Effect of composite materials on STL of a simply supported double-composite plate with enclosed air cavity.

The influence of composite materials on STL through a finite simply supported double-composite plate is studied in this section by selecting four types of composite materials: Boron/Epoxy, Glass/Epoxy, Graphite/Epoxy, and Kevlar/Epoxy. The laminated composite configuration of the bottom and the upper faceplates is $[0/90/0/90]_s$. The mechanical properties are shown in Table 1, the air speed of sound, the air density and the initial amplitude of the incident sound are presented in the above section 4.1. The dimensions of the double-plates are shown in section 4.3.

Figure 6 shows that the STL value of Boron/Epoxy materials is the largest compared to the remaining materials and the STL value of Kevlar/Epoxy materials is the smallest at frequencies lower than 100Hz because in this region surface density is the deciding factor (the stiffness-control zone). At frequencies greater than 100Hz, the STL value of Glass/Epoxy material is larger than other materials when it passes the plate-air cavity-plate resonance and the STL curves of the four materials operate according to specific rules when the plate-air cavity-plate resonance is synchronized.

5. CONCLUSIONS

In this investigation, a model was developed for the sound transmission loss through a finite double-laminated composite plate with simply supported boundary conditions excited by a plane sound wave that varying harmonically. The analytical model has been validated by comparing the present results of STL with previously published data on the double-plates. The influence of several key system parameters on STL including the plate dimensions, the laminate configurations, the boundary conditions, and the composite materials are systematically examined. From the results obtained, some conclusions can be drawn:

- The theoretical predictions are in good agreement with existing results.

- The effect of the plate dimensions on STL is particularly strong for the finite systems at low-frequency range, which is useful when designing simply supported sound insulation the composite double-plates.
- For the graphite/epoxy double-composite plate, the plies being arranged in a $[90/90/90/90]_s$ pattern of the bottom and upper plates appear to outperform other considered lamination schemes in terms of sound insulation.
- The surface density of composite materials influences considerably on STL of finite simply supported double-composite plates.
- The comparison of the STL versus frequency with the two different boundary conditions suggests that the STL values of the clamped system are distinctly higher than those of the simply supported system, especially in the lower frequency range.

Acknowledgments: This research is funded by the Vietnam National Foundation for Science and Technology Development (NAFOSTED) under grant number: 107.02-2018.07.

REFERENCES

1. Maidanik G. - Response of ribbed panels to reverberant acoustic fields, J. Acoust. Soc. Am. **34** (1962) 809–826.
2. Ruzzene M. - Vibration and sound radiation of sandwich beams with honeycomb truss core, J. Sound Vib. **277** (2004) 741–763.
3. London A. - Transmission of reverberant sound through double walls. J. Acoust. Soc. Am. **22** (1950) 270–279.
4. Carneal J. P. and Fuller C. R. - An analytical and experimental investigation of active structural acoustic control of noise transmission through double panel systems, J. Sound Vib. **272** (2004) 749–771.
5. Chazot J. D. and Guyader J. L. - Prediction of transmission loss of double panels with a patch-mobility method, J. Acoust. Soc. Am. **121** (2007) 267–278.
6. Bao C. and Pan J. - Experimental study of different approaches for active control of sound transmission through double walls, J. Acoust. Soc. Am. **102** (1997) 1664–1670.
7. Sgard F. C., Atalla N. and Nicolas J. - A numerical model for the low-frequency diffuse field sound transmission loss of double-wall sound barriers with elastic porous linings, J. Acoust. Soc. Am. **108** (2000) 2865–2872.
8. Villot M., Guigou C. and Gagliardini L. - Predicting the acoustical radiation of a finite size multi-layered structures by applying spatial windowing on infinite structures, J. Sound Vib. **245** (2001) 433–455.
9. Brouard B., Lafarge D. and Allard J. F. - A general method of modelling sound propagation in layered media, J. Sound Vib. **183** (1) (1995) 129–142.
10. Lauriks W., Mees P. and Allard J. F. - The acoustic transmission through layered systems, J. Sound Vib. **155** (1) (1992) 125–132.
11. Larbi W., Deü J.F. and R. Ohayon. - Vibroacoustic analysis of double-wall sandwich panels with viscoelastic core, Computers and Structures, **174** (2016) 92-103.
12. Panneton R. and Atalla N. - Numerical prediction of sound transmission through finite multilayer systems with poroelastic materials. J. Acoust. Soc. Am. **100** (1996) 346-354.

13. Chonan S. and Kugo Y. - Acoustic design of a three Layered plate with high sound interception, J. Sound Vib. **89** (2) (1991) 792–798.
14. Kang H. J., Ih J. G. and Kim J. S. - Prediction of sound transmission loss through multilayered panels by using Gaussian distribution of directional incident energy, J. Acoust Soc. Am. **107** (3) (2000) 1413–1420.
15. Bolton J. S., Shiau N. M. and Kang Y. J. - Sound transmission through multi-panel structures lined with elastic porous materials, J. Sound. Vib. **191** (3) (1996) 317–347.
16. Leppington F. G., Broadbent E. G. and Butler G. F. - Transmission of sound through a pair of rectangular elastic plates, Ima J. Appl. Math **71** (6) (2006), pp.940–955.
17. Lu T. J. and Xin F. X. - Vibro-acoustics of Lightweight Sandwich. Science Press Beijing and Springer-Verlag Berlin Heidenberg, 2014.
18. Thinh T. I. and Thanh P. N. - Vibro-acoustic response of an orthotropic composite laminated plate, Proceedings of National Conference on Mechanics, Ha Noi, 2017, pp. 1142-1150.
19. Pellicier A. and Trompette N. - A review of analytical methods, based on the wave approach, to compute partitions transmission loss, Applied Acoustics **68** (2007) 1192–1212.
20. Frampton K. D. - The effect of flow-induced coupling on sound radiation from convected fluid loaded plates, J. Acoust. Soc. Am. **117** (2005) 1129–1137.
21. Leissa A. W. - Vibration of plates. Acoustical Society of America, New York, 1993.
22. Howe M. S. and Shah P. L. - Influence of mean flow on boundary layer generated interior noise, J. Acoust. Soc. Am. **99** (1996) 3401–3411.
23. Frampton K. D. - The effect of flow-induced coupling on sound radiation from convected fluid loaded plates, J. Acoust. Soc. Am. **117** (2005) 1129–1137.
24. Reddy J. N. - Mechanics of laminated composite plates and shells, Theory and Analysis, Second edition, CRC Press, 2004.